Inorg. Chem. **2008**, *47*, 5048−5054

Spectroscopic Effects of Excited-State Coupling in a Tetragonal Chromium(III) Complex

Rémi Beaulac and Christian Reber*

Département de chimie, Université de Montréal, Montréal, Québec, Canada

Received November 20, 2007

Detailed low-temperature single-crystal polarized absorption and luminescence spectra of $Cs_2[CrCl_2(H_2O)_4]Cl_3$ are reported. The luminescence spectrum is a broad band with a maximum at 11 800 cm^{-1}, indicating that the *trans*-$[CrCl_2(H_2O)_4]^+$ complex emits from a quartet excited state. The resolved vibronic structure reveals a progression in a nontotally symmetric 445 cm^{-1} b_{1g} mode, a manifestation of a Jahn−Teller effect in the emitting state. The absorption spectrum shows completely linearly polarized, magnetic-dipole-allowed electronic origins, defining the tetragonal splitting of the states originating from $^4T_{2g}$ (O_h). An energy gap of approximately 800 cm^{-1} is observed between the electronic origins of the emitting state and the onset of the π-polarized absorption spectrum. Both Jahn−Teller and spin−orbit couplings in the orbitally degenerate ^4E_g (D_{4h}) state are necessary to account for the spectroscopic observations.

1. Introduction

Many chemical processes, such as electron and energy transfer and photochemical reactions, require detailed knowledge of excited-state properties.[1–5] Excited states are often close in energy, and coupling between states can have a significant influence on their characteristics. The spectroscopic investigation of coupled states is a challenge because the high density of excited states often leads to unresolved spectra, precluding detailed characterization of the manifold. Numerous reports on different chemical systems underscore the general interest of the problem and the experimental challenge that it represents.[6–18]

A recently discovered category of coupled states is the excited-state mixed-valence concept explored in detail by Zink, Nelsen, and co-workers.[8–13] The intensities of absorption transitions to the set of vibronically coupled states depend strongly on the sign of the coupling constant. The systems in these studies were generally characterized with unresolved absorption spectra and resonance Raman intensities.

Polarized absorption spectroscopy is an invaluable tool to probe many high-symmetry systems,[19,20] and polarization selection rules can be derived that help to unambiguously assign the observed transitions, leading to detailed insight

* To whom correspondence should be addressed. E-mail: reber@chimie.umontreal.ca. Tel.: (514) 343-7332. Fax: (514) 343-7586.

(1) Butler, L. J. *Annu. Rev. Phys. Chem.* **1998**, *49*, 125–171.
(2) Conroy, D.; Aristov, V.; Feng, L.; Sanov, A.; Reisler, H. *Acc. Chem. Res.* **2001**, *34*, 625–632.
(3) Plastina, F.; Piperno, F. *J. Opt. B: Quantum Semiclassical Opt.* **2000**, *2*, 140–143.
(4) Dixon, R. N.; Hwang, D. W.; Yang, X. F.; Harich, S.; Lin, J. J.; Yang, X. *Science* **1999**, *285*, 1249–1253.
(5) Bernardi, F.; Olivucci, M.; Robb, M. A. *Chem. Soc. Rev.* **1996**, *25*, 321–328.
(6) Preston, D. M.; Güntner, W.; Lechner, A.; Gliemann, G.; Zink, J. I. *J. Am. Chem. Soc.* **1988**, *110*, 5628–5633.
(7) Wexler, D.; Zink, J. I.; Reber, C. *J. Phys. Chem.* **1992**, *96*, 8757–8765.
(8) Lockard, J. V.; Zink, J. I.; Konradsson, A. E.; Weaver, M. N.; Nelsen, S. F. *J. Am. Chem. Soc.* **2003**, *125*, 13471–13480.
(9) Bailey, S. E.; Zink, J. I.; Nelsen, S. F. *J. Am. Chem. Soc.* **2003**, *125*, 5939–5947.
(10) Lockard, J. V.; Zink, J. I.; Trieber, D. A., II; Konradsson, A. E.; Weaver, M. N.; Nelsen, S. F. *J. Phys. Chem. A* **2005**, *109*, 1205–1215.
(11) Lockard, J. V.; Valverde, G.; Neuhauser, D.; Zink, J. I.; Luo, Y.; Weaver, M. N.; Nelsen, S. F. *J. Phys. Chem. A* **2006**, *110*, 57–66.
(12) Nelsen, S. F.; Weaver, M. N.; Luo, Y.; Lockard, J. V.; Zink, J. I. *Chem. Phys.* **2006**, *324*, 195–201.
(13) Nelsen, S. F.; Luo, Y.; Weaver, M. N.; Lockard, J. V.; Zink, J. I. *J. Org. Chem.* **2006**, *71*, 4286–4295.
(14) Bussière, G.; Reber, C. *J. Am. Chem. Soc.* **1998**, *120*, 6306–6315.
(15) Bussière, G.; Beaulac, R.; Cardinal-David, B.; Reber, C. *Coord. Chem. Rev.* **2001**, *219–221*, 509–543.
(16) Pelletier, Y.; Reber, C. *Inorg. Chem.* **1997**, *36*, 721–728.
(17) Wheeler, D. E.; McCusker, J. K. *Inorg. Chem.* **1998**, *37*, 2296–2307.
(18) Damrauer, N. H.; Boussie, T. R.; Devenney, M.; McCusker, J. K. *J. Am. Chem. Soc.* **1997**, *119*, 8253–8268.
(19) Hitchman, M. A.; Riley, M. J. Polarized Absorption Spectroscopy. In *Inorganic Electronic Structure and Spectroscopy*; Solomon, E. I., Lever, A. B. P., Eds.; John Wiley & Sons: New York, 1999; Vol. *1*.

10.1021/ic702281k CCC: $40.75
Published on Web 05/10/2008

on the electronic structure of the systems studied.[20] Tetragonal and trigonal symmetries are particularly well suited for such studies.

Transition-metal complexes are ideal systems to probe excited-state coupling because of their rich electronic structure being easily modified by simple chemistry. In particular, the first excited states of six-coordinate chromium(III) complexes have been thoroughly studied because of their interesting photophysical and photochemical behavior.[21–25] Recently, reports on the ultrafast dynamics of the formation of the long-lived ^2E_g excited state of a chromium(III) complex have emphasized the importance of coupling in these systems.[26,27] The lowest-energy quartet excited state of these complexes is often close in energy to the extensively studied ^2E_g state and its excited-state structure has attracted interest from many groups.[28–34] The reported absorption and luminescence spectra of high-symmetry (O_h) complexes clearly show distortions along multiple normal coordinates, but obviously no polarization effects were observed in cubic symmetry.

We present well-resolved polarized absorption and luminescence spectra of a tetragonal chromium(III) complex, *trans*-$[CrCl_2(H_2O)_4]^+$. Our spectroscopic results show that this complex is one of the rare cases with luminescence from the quartet excited state. The high resolution of the origins of the electronic transitions in luminescence and in polarized absorption spectra makes it possible to unambiguously assign each transition and to rigorously analyze the observed polarizations.

2. Experimental Section

Complexes were prepared as described in the literature.[35] The space group of the crystals is $C2/m$, with the Cr^{3+} ion located on a site with almost exact D_{4h} symmetry, with all ligand−metal−ligand angles deviating by less than 1° from 90°.[35–37] Samples for spectroscopic measurements were cooled in a helium gas continuous-flow cryostat (Oxford CF-1204). Steady-state luminescence measurements were performed on a microscope spectrometer (Renishaw 3000), using the 514.5 nm line of an argon ion laser to excite the sample. A 90° adaptor specially designed to fit the microscope (Renishaw macro sampling set) was used in order to orient the microscope objective toward a cryostat window and to collect emitted light. Absorption measurements were made on a Varian Cary 5E UV−vis−NIR spectrometer. A set of Glan-Taylor polarizers was used to linearly polarize the light. Spectra were recorded with light polarized parallel to the extinction axes of the crystals, as determined under a polarizing microscope. Angular overlap model (AOM) calculations were performed with the *AOMX* program, version 9.6.96.[38]

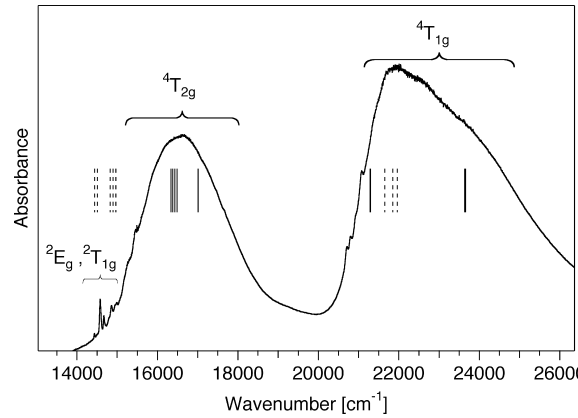

Figure 1. Unpolarized absorption spectrum of $Cs_2[CrCl_2(H_2O)_4]Cl_3$ at 5 K with O_h symmetry labels. The vertical lines indicate calculated energies of all electronic states obtained with the AOM parameters in Table 1 in the energy range of the experimental spectrum. Dotted and solid vertical lines denote calculated energies of doublet and quartet states, respectively.

3. Results

3.1. Polarized Absorption Spectroscopy. Figure 1 shows the unpolarized absorption spectrum of $Cs_2[CrCl_2(H_2O)_4]Cl_3$ at 5 K. The spectrum consists of two broad bands that are readily assigned as the first two spin-allowed d−d transitions in octahedral point-group symmetry, indicating that the overall ligand field for the title complex is not very far from O_h. The lower actual point-group symmetry does not lead to multiple band maxima, and the energy differences from lifted degeneracies in D_{4h} point-group symmetry appear to be smaller than the widths of the observed absorption bands. Narrow transitions are seen on the low-energy side of each broad band and are assigned as spin-forbidden transitions to doublet excited states. The most intense absorption features corresponding to these transitions are those at lowest energy, around 14 500 cm^{-1}, creating an energy gap on the order of 800 cm^{-1}, denoted by the double-headed arrow in Figure 3. A second set of forbidden transitions is observed at approximately 21 000 cm^{-1}. Figure 2 shows the polarized spectra of $Cs_2[Cr(D_2O)_4Cl_2]Cl_3$ in the region of the first broad-band transition.

The overall band shapes in σ and π polarizations and the dichroic ratios of all transitions are similar to those measured by McCarthy et al. for $Cs_2[CrCl_2(H_2O)_4]Cl_3$.[35] The system

(20) Ferguson, J. *Prog. Inorg. Chem.* **1970**, *12*, 159–293.
(21) Kirk, A. D. *Chem. Rev.* **1999**, *99*, 1607–1640.
(22) Forster, L. S. *Chem. Rev.* **1990**, *90*, 331–353.
(23) Adamson, A. W. *J. Phys. Chem.* **1967**, *71*, 798–808.
(24) Kane-Maguire, N. A. *Top. Curr. Chem.* **2007**, *280*, 37–67.
(25) Adamson, A. W., Fleischauer, P. D., Eds. *Concepts of Inorganic Photochemistry*; Wiley: New York, 1975.
(26) Juban, E. A.; McCusker, J. K. *J. Am. Chem. Soc.* **2005**, *127*, 6857–6865.
(27) Juban, E.; Smeigh, A. L.; Monat, J. E.; McCusker, J. K. *Coord. Chem. Rev.* **2006**, *250*, 1783–1791.
(28) Wilson, R. B.; Solomon, E. I. *Inorg. Chem.* **1978**, *17*, 1729–1736.
(29) Güdel, H. U.; Snellgrove, T. R. *Inorg. Chem.* **1978**, *17*, 1617–1620.
(30) Wenger, O. S.; Valiente, R.; Güdel, H. U. *J. Chem. Phys.* **2001**, *115*, 3819–3826.
(31) Wenger, O. S.; Güdel, H. U. *J. Chem. Phys.* **2001**, *114*, 5832–5841.
(32) Gilardoni, F.; Weber, J.; Bellafrouh, K.; Daul, C. A.; Güdel, H. U. *J. Chem. Phys.* **1996**, *104*, 7624–7632.
(33) Schatschneider, B.; Perumareddi, J. R. *Inorg. Chim. Acta* **2005**, *358*, 4571–4574.
(34) Knochenmuss, R. D.; Reber, C.; Rajasekharan, M. V.; Güdel, H. U. *J. Chem. Phys.* **1986**, *85*, 4280–4289.
(35) McCarthy, P. J.; Lauffenburger, J. J.; Skonezny, P. M.; Rohrer, D. C. *Inorg. Chem.* **1981**, *20*, 1566–1570.
(36) Nyburg, S. C.; Soptrjanov, B.; Stefov, V.; Petrusevski, V. M. *Inorg. Chem.* **1997**, *36*, 2248–2251.
(37) Neumann, E.; Stefov, V.; Soptrjanov, B.; Engelen, B.; Lutz, H. D. *J. Mol. Struct.* **2004**, *708*, 105–111.
(38) Adamsky, H.; Schönherr, T.; Atanasov, M. A. AOMX: Angular Overlap Model Computation. In *Comprehensive Coordination Chemistry II*; McCleverty, J. A., Meyer, T. J., Eds.; Elsevier: Oxford, U.K., 2004; Vol. *2*.

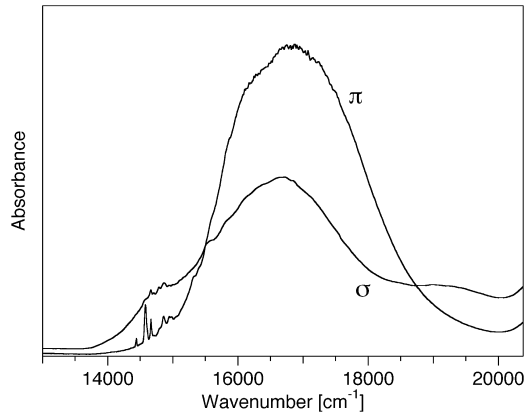

Figure 2. Linearly polarized absorption spectra of $Cs_2[Cr(D_2O)_4Cl_2]Cl_3$ at 5 K, in the region of the lowest-energy d−d transitions.

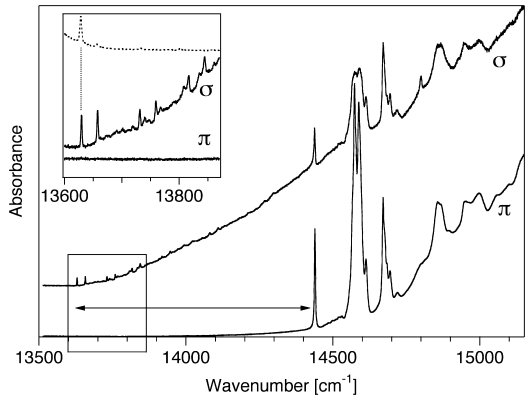

Figure 3. Linearly polarized absorption spectra of $Cs_2[CrCl_2(H_2O)_4]Cl_3$ at 5 K, in the origin region of the lowest-energy broad-band transition and of the first spin-forbidden transitions. The onset of the 5 K emission spectrum is shown in the inset (broken line), along with the onset of the two linearly polarized absorption spectra. The double arrow indicates the energy gap between the onsets in both polarizations.

of bands illustrated in Figure 2 is about twice as intense in π than in σ polarization. A clearly visible difference between the two spectra is observed at the low-energy side of the band. The onset of the broad band in σ polarization occurs on the high-energy side of the origin at 13 630 cm^{-1}, whereas no noticeable intensity is seen in π polarization before the set of forbidden transitions at around 14 500 cm^{-1}. This difference in the two polarizations is also observed for the nondeuterated complex, as shown in Figure 3, which gives the first detailed view of this region containing both broad-band and narrow-line transitions. The well-resolved lowest-energy transitions, shown in the inset of Figure 3, illustrate that the electronic origins of the broad-band centered around 16 500 cm^{-1} in Figure 1 occur at lower energy than the narrow spin-forbidden transitions at approximately 14 500 cm^{-1}. These very narrow origins observed between 13 600 and 13 800 cm^{-1} are completely σ-polarized and are assigned as magnetic-dipole (MD)-allowed electronic origins of the lowest-energy spin-allowed d−d transitions. The comparison with the luminescence spectrum presented in the following section confirms this assignment.

3.2. Luminescence Spectroscopy. The luminescence spectrum of $Cs_2[CrCl_2(H_2O)_4]Cl_3$ measured at 5 K is shown in Figure 4a. A broad luminescence band with a width at half-height of 1700 cm^{-1} is observed, similar to the

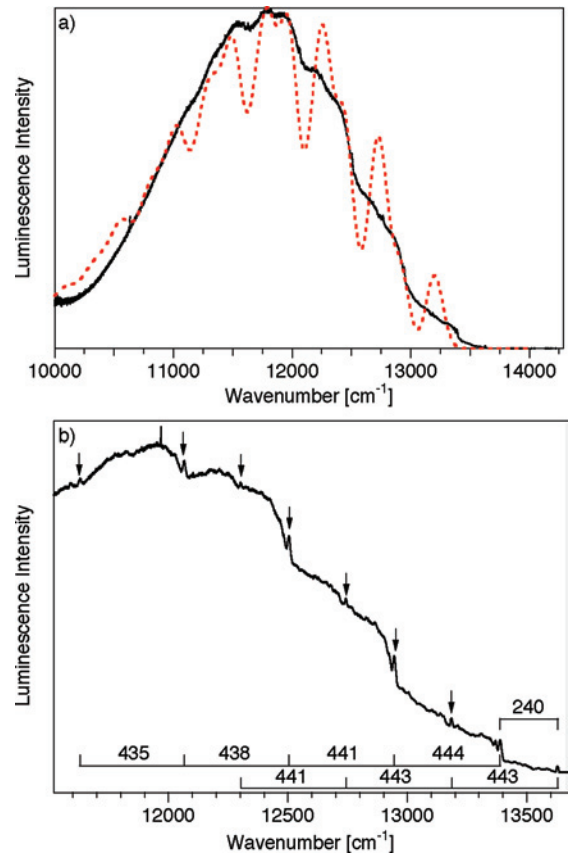

Figure 4. (a) Luminescence spectrum (black solid line) and calculated luminescence spectrum (red dotted line) of $Cs_2[CrCl_2(H_2O)_4]Cl_3$ at 5 K. (b) Onset of the experimental spectrum shown in part a, with arrows denoting peaks forming the two vibronic progressions with average intervals of 445 cm^{-1}, each built on origins separated by 240 cm^{-1}. Vibronic intervals in cm^{-1} units are given at the bottom of the figure.

luminescence spectra of weak-field octahedral chromium(III) complexes such as $[CrCl_6]^{3-}$,[29–31,34] suggesting that emission originates from a quartet excited state rather than the usual narrow-band spin-forbidden emission observed for aquo complexes of chromium(III).[22] The highest-energy narrow peak in the luminescence spectrum is located at 13 630 cm^{-1}, identical in energy to the lowest-energy narrow absorption peak shown in Figure 3. This comparison shows unambiguously that the observed luminescence originates from the *trans*-$[CrCl_2(H_2O)_4]^+$ complex and not from an impurity acting as a trap.

The luminescence spectrum of $Cs_2[CrCl_2(H_2O)_4]Cl_3$ shows a few narrow, well-resolved peaks located on the high-energy side of the band, as illustrated by the arrows in Figure 4b. These peaks form two vibronic progressions with average intervals of 445 cm^{-1}, with each progression built on a different origin. One set of peaks is built on the electronic origin located at 13 630 cm^{-1}; the other set of peaks is built on a vibronic origin located 240 cm^{-1} lower in energy than the electronic origin. Such vibronic origins are the most efficient mechanism to obtaining an electron-dipole (ED) intensity for d−d transitions in complexes with inversion symmetry. Vibronic origins always involve odd-parity vibrational modes, typically observed in the IR spectrum. The IR spectrum of the title complex has been reported and

Scheme 1

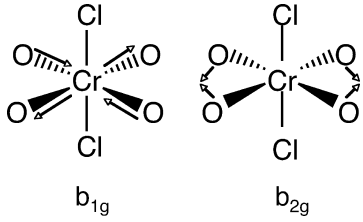

contains a band at 240 cm^{-1}.[39] The two vibronic progressions show a slight reduction of the spacing between members toward lower energy, possibly a result of the anharmonicity of the ground-state potential-energy surface along the normal coordinate of the mode forming the progressions. According to a published analysis of the Raman spectrum, this mode is assigned to the b_{1g} M−O stretching mode (cf. Scheme 1), observed at a frequency of 445 cm^{-1}.[39] The observation of progressions involving nontotally symmetric modes in the luminescence spectrum suggests that the emitting state is Jahn−Teller-distorted, as discussed in the following section.

4. Discussion

4.1. Band Assignments for the Tetragonal Complex. The splitting of the electronic states due to the lowering of the symmetry from O_h to D_{4h} is qualitatively predicted by ligand-field theory.[40] A schematic view of the tetragonal splitting of the first excited states is illustrated in Figure 5. According to the spectrochemical series, the ligand-field strength of the *trans*-$[CrCl_2(H_2O)_4]^+$ complex is slightly weaker along the tetragonal axis than in the plane containing the four aqua ligands. In this case, the ^4E_g component arising from $^4T_{2g}$ (O_h) is predicted to be lower in energy than the $^4B_{2g}$ component.[41] The $^4E_g \leftarrow {}^4B_{1g}$ transition is allowed in σ polarization for the MD mechanism and forbidden in π polarization, as observed in the experimental absorption spectum. In contrast, the $^4B_{2g} \leftarrow {}^4B_{1g}$ MD transition is forbidden in σ polarization and allowed in π polarization, as shown in Figure 5. The narrow peak observed at 13 630 cm^{-1} in the absorption (Figure 3) and luminescence (Figure 4) spectra is assigned as the lowest-energy electronic origin of the quartet system. It is completely σ-polarized and is thus assigned as the $^4E_g \leftarrow {}^4B_{1g}$ transition, confirming experimentally that the ^4E_g state is lower in energy than the $^4B_{1g}$ state. To the best of our knowledge, this is the first determination of the energetic order of excited states in a chromium(III) complex deviating from O_h symmetry based on the polarization of electronic origins. The assignment of the emitting state is further confirmed by the observation of a progression involving the nontotally symmetric b_{1g} mode in the luminescence spectrum. Such progressions can only be observed for orbitally degenerate emitting states undergoing Jahn−Teller distortions, which further excludes the possibility that the nondegenerate $^4B_{2g}$ state is the lowest-energy component of $^4T_{2g}$ (O_h). The analysis of polarized absorption origins and vibronic structure in the luminescence spectrum thus confirms unambiguously the ^4E_g assignment of the lowest-energy quartet excited state.

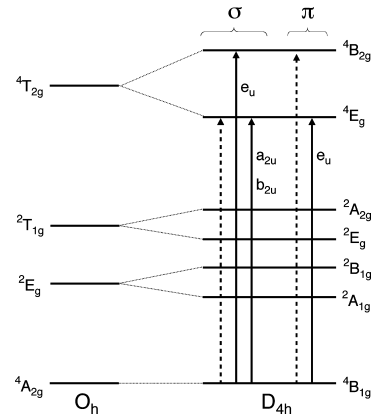

Figure 5. Correlation diagram illustrating the tetragonal splitting of the first excited states of a nearly octahedral d^3 system. Dotted arrows represent MD-allowed transitions and solid arrows indicate ED-allowed transitions, alongside with the necessary ungerade parity vibrational modes needed to break the Laporte rule. The energetic order of states and ordinate scale are not quantitative.

Table 1. AOM Parameters for $Cs_2[CrCl_2(H_2O)_4]Cl_3$[a]

parameter	value [cm^{-1}]	Euler angles	values [deg]
e_σ(O)	7000	Θ_{Cl_1}, Φ_{Cl_1}, Ψ_{Cl_1}	0.0, 0.0, 0.0
$e_{\pi\|\|}$(O)	500	Θ_{Cl_2}, Φ_{Cl_2}, Ψ_{Cl_2}	180.0, 0.0, 0.0
$e_{\pi\perp}$(O)	1000	Θ_{O_1}, Φ_{O_1}, Ψ_{O_1}	90.0, 0.0, 0.0
e_σ(Cl)	6000	Θ_{O_2}, Φ_{O_2}, Ψ_{O_2}	90.0, 90.0, 0.0
e_π(Cl)	1000	Θ_{O_3}, Φ_{O_3}, Ψ_{O_3}	90.0, 180.0, 0.0
B	599 (1030)	Θ_{O_4}, Φ_{O_4}, Ψ_{O_4}	90.0, 270.0, 0.0
C	3332 (3850)		
ζ	171 (209)		

[a] Free-ion parameters for B, C, and ζ are given in parentheses.[45]

A detailed assignment of the spin-forbidden transitions is not possible. The systems of narrow absorption bands around 14 500 cm^{-1} involve both low-symmetry ^2E_g and $^2T_{1g}$ origins split by spin−orbit interaction between quartet and doublet states and probably also vibronic origins. It is, nevertheless, clear that the lowest-energy narrow peak in this region, located at 14 439 cm^{-1}, corresponds to a spin-forbidden transition and not to a vibronic origin built on the electronic origin of the $^4E_g \leftarrow {}^4B_{1g}$ transition because the same transition appears in both polarizations, whereas no common enabling mode can vibronically induce the $^4E_g \leftarrow {}^4B_{1g}$ transition in both polarizations, as shown in Figure 5. A set of AOM parameters, given in Table 1, has been obtained in order to reproduce as well as possible the energies of the observed absorption band maxima. A comparison between the experimental transition energies and calculated energy differences is given in Table 2; the positions of the calculated transitions are also shown as vertical bars in Figure 1. The calculation indicates different tetragonal splittings for the $^4T_{2g}$ and $^4T_{1g}$ (O_h) states. The calculated splitting of the $^4T_{1g}$ state is almost 3 times larger than that of the $^4T_{2g}$ state (Table 2), providing a rationale for the much larger observed width of the higher-energy broad band shown in Figure 1. The molecular planes of the water ligands were positioned parallel to the C_4 molecular axis, and π anisotropy is included via the different values for $e_{\pi\perp}$(O) and $e_{\pi\|}$(O) in Table 1. This anisotropy has

(39) Michalska-Fong, D.; McCarthy, P. J.; Nakamoto, K. *Spectrochim. Acta* **1983**, *39A*, 835–842.
(40) Ballhausen, C. J. *Introduction to Ligand-Field Theory*; McGraw-Hill: New York, 1962.
(41) Webb, G. A. *Coord. Chem. Rev.* **1969**, *4*, 107–145.

Table 2. Calculated and Observed Energies for the Ground State and Lowest-Energy Excited States of $Cs_2[CrCl_2(H_2O)_4]Cl_3$, Using the Parameters in Table 1

state				
O_h	D_{4h}	D_{4h}'	calcd energy[a] [cm^{-1}]	obsd energy [cm^{-1}]
$^4A_{2g}$	$^4B_{1g}$	Γ_7	0	0
		Γ_6	0.037	
^2E_g	$^2A_{1g}$	Γ_6	14 438	14 438
	$^2B_{1g}$	Γ_7	14 505	
$^2T_{1g}$	^2E_g	Γ_7	14 822	
		Γ_6	14 898	14 800−15 100
	$^2A_{2g}$	Γ_6	14 966	
$^4T_{2g}$	^4E_g	Γ_7	16 340	16 580[a]
		Γ_7	16 382	
		Γ_6	16 432	
		Γ_6	16 489	
	$^4B_{2g}$	Γ_6	17 008	
		Γ_7	17 015	
$^4T_{1g}$	$^4A_{2g}$	Γ_6, Γ_7	21 297[b]	21 900[a]
	^4E_g	$2\Gamma_6$, $2\Gamma_7$	23 636[b]	23 650[a]

[a] Absorption band maximum. [b] Calculated with parameters in Table 1, $\zeta = 0$.

been shown to be important by electronic structure calculations on *trans*-$[TiCl_2(H_2O)_4]^+$ and *trans*-$[VCl_2(H_2O)_4]^+$ and also for a number of other metal−aquo complexes.[42–44]

The selection rules in Figure 5 show that the $^4B_{2g} \leftarrow {}^4B_{1g}$ transition is strictly ED-forbidden in π polarization. The π-polarized band shown in Figure 2 must therefore correspond to a vibronically ED-allowed transition to the ^4E_g state because it is much too intense to correspond only to the MD-allowed $^4B_{2g} \leftarrow {}^4B_{1g}$ electronic transition. The exact positions of the $^4E_g \leftarrow {}^4B_{1g}$ electronic origins are precisely known from the σ-polarized absorption spectrum and the luminescence spectrum (inset of Figure 3). The π-polarized absorption spectrum reveals that no resolved vibronic origins are observed lower in energy than the first transition to a doublet state, located approximately 800 cm^{-1} higher in energy than the lowest-energy electronic origin of the $^4E_g \leftarrow {}^4B_{1g}$ transition. This energy difference indicates that the vibronic origin(s) giving rise to the intensity of the whole band in π polarization would have to involve vibrational frequencies of at least 800 cm^{-1}, a value much too high to correspond to any of the metal−ligand modes.[39] Because metal−ligand vibrations are the only modes that can lead to sizable coupling of the even-parity d states with higher-energy odd-parity states, we are led to the conclusion that the intensity absorption in π polarization cannot originate from such vibronic coupling interactions, for then a much smaller gap between the zero-phonon lines and the vibronic origins should be observed. The origin of the overall intensity of absorption in π polarization and of the unusually large energy gap between the σ-polarized electronic origins and the onset of the band in π polarization is discussed in the following section in terms of Jahn−Teller distortions and spin−orbit coupling acting on the ^4E_g state.

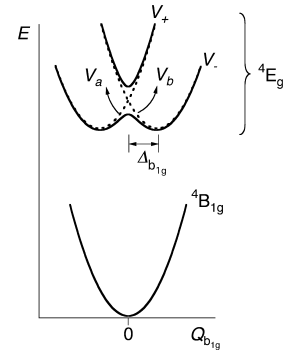

Figure 6. Representation of the electronic system for a doubly degenerate excited state under the influence of $E_g \otimes b_{1g}$ Jahn−Teller coupling and spin−orbit coupling. The diabatic states V_a and V_b (before spin−orbit coupling) are shown as dotted lines, and the adiabatic states V_+ and V_- (after spin−orbit coupling) are given by solid lines.

4.2. Potential-Energy Surfaces of the Lowest-Energy ^4E_g Excited State. The detailed polarized absorption spectra in Figure 3 and the luminescence spectra in Figure 4 provide information beyond the assignment of the lowest-energy excited state as ^4E_g in D_{4h} point-group symmetry. In this section, we focus on the vibronic progressions observed in the luminescence spectrum and on the lack of intensity in the π-polarized absorption spectrum for the lowest-energy transition shown in the inset of Figure 3. In the D_{4h} point group, a degenerate E_g state can be distorted along the a_{1g}, b_{1g}, and b_{2g} normal coordinates. The Jahn−Teller active b_{1g} and b_{2g} modes are shown in Scheme 1. The b_{2g} bending mode is not observed as a progression in the luminescence spectrum, and it is expected to be less important for the Jahn−Teller splitting of the ^4E_g state than the b_{1g} mode because the $^4E_g \leftarrow {}^4B_{1g}$ transition implies a change in the population of d orbitals mainly directed along the metal−ligand bonds. In the following, we apply a model with as few adjustable parameters as possible. It therefore involves only the b_{1g} and a_{1g} modes. Vibronic coupling with the b_{1g} mode splits the ^4E_g state into two surfaces whose minima are symmetrically displaced to each side of the ground-state equilibrium geometry along the b_{1g} coordinate, as illustrated by the two dotted curves in Figure 6. In the absence of vibronic coupling with the b_{2g} mode ($E \otimes b_1$ static Jahn−Teller effect[46]), these two surfaces are orthogonal and their vibrational levels are degenerate. This coupling scheme alone then cannot account for the absence of intensity observed in the π-polarized absorption spectrum, as illustrated by the double arrow in Figure 3.

Spin−orbit coupling also exists between the two components of the E_g state, leading to a situation with two states separated in energy, as shown by the two solid excited-state potential-energy curves in Figure 6. The harmonic excited-state potential-energy curves given by the dotted lines are defined along the b_{1g} Jahn−Teller active coordinate in Figure 6 by

$$V_{a,b}(Q_{b_{1g}}) = \frac{1}{2}k_{b_{1g}}(Q_{b_{1g}} \pm \Delta_{b_{1g}})^2 \quad (1)$$

The ^4E_g excited state can also be offset along the totally symmetric normal coordinates:

(42) Tregenna-Piggott, P. L. W.; Spichiger, D.; Carver, G.; Frey, B.; Meier, R.; Weihe, H.; Cowan, J. A.; McIntyre, G. J.; Zahn, G.; Barra, A.-L. *Inorg. Chem.* **2004**, *43*, 8049–8060.
(43) Tregenna-Piggott, P. L. W.; Weihe, H.; Barra, A.-L. *Inorg. Chem.* **2003**, *42*, 8504–8508.
(44) Tregenna-Piggott, P. L. W.; Best, S. P.; Güdel, H. U.; Weihe, H.; Wilson, C. C. *J. Solid State Chem.* **1999**, *145*, 460–470.
(45) Griffith, J. S. *The Theory of Transition-Metal Ions*; University Press: Cambridge, U.K., 1961.

$$V_{a,b}(Q_{a_{1g}}) = \frac{1}{2}k_{a_{1g}}(Q_{a_{1g}} - \Delta_{a_{1g}})^2 \quad (2)$$

We use dimensionless units for the normal coordinates Q_i, and k_i denote vibrational frequencies in cm^{-1} units. Identical frequencies were used for the ground-state and excited-state potential-energy surfaces. Spin−orbit coupling is assumed to be coordinate-independent and represented by the effective constant λ, leading to the following system of coupled excited-state potential-energy surfaces:[7–16]

$$\hat{V}_{^4E_g} = \begin{pmatrix} V_a & \lambda \\ \lambda & V_b \end{pmatrix} \quad (3)$$

The adiabatic excited-state potential-energy curves $V_\pm$ shown as solid lines in Figure 6 are given by

$$V_\pm = \frac{V_a + V_b}{2} \pm \lambda \quad (4)$$

We note that the sign of the single coupling constant λ has no influence on the shape of the $V_\pm$ curves shown in Figure 6. Along the $Q_{b_{1g}}$ normal coordinate, the lower-energy curve of the $V_\pm$ adiabatic ensemble shows two minima at $\pm\Delta_{b_{1g}}$ and a maximum at $Q_{b_{1g}} = 0$, whereas the upper curve has a single minimum at $Q_{b_{1g}} = 0$. A single minimum is observed along the totally symmetric normal coordinate $Q_{a_{1g}}$. The parameters $\Delta_{a_{1g}}$, $\Delta_{b_{1g}}$, and λ of this model cannot be directly determined from experimental spectra and will be determined from the comparison of calculated and experimental spectra.

This model is formally identical with those used to characterize the ^4E_g excited-state potential-energy surfaces of square-planar platinum(II) and palladium(II) complexes with halide ligands,[6,16,47] which share the D_{4h} point-group symmetry with the title compound. The spectroscopic features of interest in the square-planar complexes are progressions in the b_{1g} nontotally symmetric mode in the luminescence spectra and an apparent gap in the absorption spectra between the onset of luminescence and absorption bands. These observations were analyzed in terms of coupled excited-state potential-energy surfaces defined by eqs 1–3. Our spectra offer a particularly well-defined situation because the ^4E_g symmetry of the excited state is unambiguously assigned via the polarization of resolved electronic origins observed in both absorption and luminescence spectra.

We first analyze the luminescence spectrum shown in Figure 4, where a partially resolved vibronic structure is observed. The prominent progression is the Jahn−Teller active b_{1g} stretching mode with a ground-state frequency of 445 cm^{-1}.[39] Frequencies of 490 and 289 cm^{-1} have been measured for the totally symmeric chromium−aquo and chromium−chloro stretching modes, respectively.[39] We use these three frequencies to define the potential-energy surfaces of the ground and emitting states. The luminescence spectrum is given by[48,49]

Table 3. Parameters Used To Calculate the Luminescence Spectrum Shown as a Dotted Line in Figure 4

parameter	value
E_{00} (cm^{-1})	13 200
Γ (cm^{-1})	50
$k_{a_{1g}}$ (cm^{-1}), $\Delta_{a_{1g}}$ (dim. less)	490, 1.77
$k_{a_{1g}}$ (cm^{-1}), $\Delta_{a_{1g}}$ (dim. less)	289, 1.52
$k_{b_{1g}}$ (cm^{-1}), $\Delta_{b_{1g}}$ (dim. less)	445, 1.78

$$I(\omega) = C\omega^3 \int_{-\infty}^{\infty} e^{i\omega t}\langle\varphi|\varphi(t)\rangle \, dt \quad (5)$$

$$\langle\phi|\phi(t)\rangle = \exp\left\{\sum_j \left[-\frac{\Delta_j^2}{2}(1 - e^{-ik_j t}) - \frac{ik_j t}{2}\right] - iE_{00}t - \Gamma^2 t^2\right\} \quad (6)$$

where E_{00} is the energy of the origin, k_j are the vibrational frequencies of each mode, and Γ is a phenomenological factor determining the width of each line. Our model is simplified as it does not include any low-frequency modes, and considers only intensity built on one origin, representing an effective vibronic origin. The calculated spectrum is compared to the experimental luminescence spectrum in Figure 4. In view of the simplicity of the model, the agreement is good. In particular, the model reproduces the relative intensity of the shoulders near the band maximum and the overall width of the luminescence spectrum. The errors of the Δ_j values are estimated to be less than 3%. Numerical parameters obtained from the calculation are summarized in Table 3. The spin−orbit coupling parameter λ cannot be determined from these calculations because only the excited-state potential-energy minimum is characterized by luminescence.

The Jahn−Teller stabilization of the excited state is calculated as

$$E_{JT} = \frac{1}{2}k_{b_{1g}}\Delta_{b_{1g}}^2 \quad (7)$$

A value of 705 cm^{-1} is obtained from the parameters in Table 3. Its magnitude corresponds to the apparent gap of the absorption intensity of at least 800 cm^{-1} in the π-polarized spectrum shown in the inset of Figure 3. This is in qualitative agreement with the energy gaps analyzed in square-planar complexes, where the magnitude of the gap in the absorption spectrum corresponds to the barrier height of the lower adiabatic surface shown in Figure 6. Spin−orbit coupling leads to the maximum of the lower potential-energy curve in Figure 6, and it is this feature that leads to very low absorption intensity in the region of the electronic origin, as has been explored in detail.[6,16,47] It is interesting to note that the gap is only observed in one polarization. The avoided crossing between the adiabatic potential-energy curves in Figure 6 increases the energy gap and is the likely cause for the larger gap observed than calculated from eq 7. Vibronic

(46) Bersuker, I. B.; Polinger, V. Z. *Vibronic Interactions in Molecules and Crystals*; Springer-Verlag: New York, 1989.
(47) Reber, C.; Zink, J. I. *J. Phys. Chem.* **1991**, *95*, 9151–9158.
(48) Zink, J. I. *Coord. Chem. Rev.* **2001**, *211*, 69–96.
(49) Zink, J. I.; Shin, K.-S. K. *Adv. Photochem.* **1991**, *16*, 119–214.

Table 4. Excited-State Distortions Δ_j in Dimensionless Units for the Lowest-Energy Quartet Excited State of Octahedral Chromium(III) Complexes Determined from Absorption or Luminescence Spectra with Resolved Vibronic Structure

complex	$\Delta_{a_{1g}}$	Δ_{e_g}	$\Delta_{b_{1g}}$
trans-$[CrCl_2(H_2O)_4]^{+a}$	1.7, 1.5	n/a	1.8
$[Cr(NH_3)_6]^{3+b}$	2.3	2.1	n/a
$Cs_2NaInCl_6:Cr^{3+c}$	1.8	1.6	n/a
$Cs_2NaYCl_6:Cr^{3+d}$	1.8	1.8	n/a
$Cs_2NaScCl_6:Cr^{3+e}$	1.7	1.5	n/a

[a] This work, two a_{1g} modes. [b] Reference 28. [c] Reference 29. [d] Reference 34. [e] Reference 31.

intensity mechanisms involving nonzero transition dipoles away from the equilibrium geometry are the most likely reason for the intensity in σ polarization. The polarized absorption spectra show that an energy gap cannot always be determined from unpolarized spectra. This might lead to a crucial neglect of an important feature of excited-state potential-energy surfaces. The full excited-state structure of *trans*-$[CrCl_2(H_2O)_4]^+$, including spin−orbit and possible low-symmetry splittings and all vibronic enabling modes, involves too many unknown quantities to unambiguously assign the physical origin of the observed polarizations in the region of the energy gap.

Jahn−Teller distortions of the $^4T_{2g}$ excited state have been determined for a number of octahedral chromium(III) complexes with halide and ammine ligands.[28,29,31,34] Absorption and luminescence spectra with resolved vibronic progressions involving the totally symmetric stretching mode and the Jahn−Teller active e_g stretching mode built on vibronic origins are observed at low temperature, and the intensity distributions within the progressions have been used to determine excited-state distortions.[28–31,34] Electronic structure calculations have given distortions comparable to those determined from the spectra.[32] Usually, these distortions are given in terms of Huang−Rhys parameters S_j, related to the Δ_j values in eqs 1 and 2 by[50]

$$\Delta_j = \sqrt{2S_j} \tag{8}$$

Table 4 summarizes literature values and our results for distortions in the lowest-energy quartet excited state of several chromium(III) complexes. The magnitudes of the distortions obtained from resolved vibronic progressions are similar for the series of compounds in Table 4. Our analysis with a simple model indicates that the ^4E_g excited-state Jahn−Teller distortion in the tetragonal title complex is similar in size to those reported for high-symmetry, homoleptic complexes.

Acknowledgment. Financial support from the Natural Sciences and Engineering Research Council (Canada) and the Fonds Québécois de la Recherche sur la Nature et les Technologies is acknowledged. We are grateful to Dr. Guillaume Bussière for his contribution to the spectroscopic measurements and to Étienne Lanthier, Dr. Xiao-Gang Wang, and Dr. Victor Polinger for very helpful discussions.

IC702281K

(50) Brunold, T. C.; Güdel, H. U. Luminescence Spectroscopy. In *Inorganic Electronic Structure and Spectroscopy*; Solomon, E. I., Lever, A. B. P., Eds.; John Wiley & Sons: New York, 1999; Vol. *1*.